Friction and wear of Cu-15 wt%Ni-8 wt%Sn bronze lubricated by grease at room and elevated temperature

Juanjuan Zhu[a], Le Ma[b], Rob S Dwyer-Joyce[a]

[a] The Leonardo Centre for Tribology, Department of Mechanical Engineering, University of Sheffield, Mappin Street, Sheffield, S1 3JD, UK

[b] Sorby Centre, Kroto Research Institute, North Campus, University of Sheffield, Broad Lane, Sheffield, S3 7HQ, UK

Abstract

Cu-15 wt%Ni-8 wt%Sn (CuNiSn) bronze alloy shows promising bearing performance when used in tribological applications and has attracted increasing research interest. In this work, the tribological performance of CuNiSn in terms of friction and wear were investigated in a ball-on-disc contact configuration, sliding against a Al_2O_3 ball under varying normal loads (1 and 4 N) and environmental temperatures (room temperature (~18°C) and 110 °C). Post-test characterization techniques, including optical profilometry, scanning electron microscopy (SEM), energy dispersive X-ray (EDX) and transmission electron microscopy (TEM) were adopted to characterize the wear track on the CuNiSn surface after 13500 cycles of reciprocating sliding. Both friction and wear behaviour was found to depend on the load and temperature whilst wear resistance reduced with increased temperature. A mechanically mixed layer (MML) and plastic deformation layer (PDL) were characterized by TEM micrographs of the cross-section from the wear track. Under 4 N load, a 1-1.5 µm thick tribolayer was developed during sliding at room temperature compared with a 200-300 nm tribolayer at 110 °C. The friction and wear mechanisms were largely dominated by properties of the tribolayers which were initially associated with and affected by load and temperature.

Keywords: CuNiSn bronze alloy, bearing performance, tribolayer, friction, wear mechanism

1. Introduction

Bronze alloys are widely used as bearing materials due to their favourable tribological performance with or without lubrication in addition to good resistance to shock and impact. Cu-15 wt%Ni-8 wt%Sn (CuNiSn), commercially known as ToughMet 3 (C72900, Materion Corporation), is a newly invented spinodal bronze alloy. The CuNiSn has shown exceptional bearing performance, including lower friction and wear characteristics, improved corrosion resistance, and enhanced toughness, which make the material a promising candidate for demanding applications, such as aircraft landing gear bushings or heavy equipment bearings in aerospace, automotive, oil or gas industries [1-5]. Compared to conventional moderate strength aluminium bronze, CuNiSn is considered to be an improved bearing alloy as it combines high strength and good tribological characteristics. For example, the AT alloy (hot wrought and spinodally hardened CuNiSn) has a 0.2% offset yield strength of 758 MPa that is significantly higher than that of standard complex aluminium bronze alloys AMS 4590, 621MPa. This provides an important potential for weight reduction particularly for the aerospace industry where weight is a critical design parameter [2, 6].

As a modern bearing material, CuNiSn alloy has emerged as a material of choice for bushings or plain bearing components. A systematic mechanical and tribological properties database for CuNiSn is therefore required. Ilangovan et al. studied the hardness and wear of sand cast CuNiSn (Cu-7 wt%Ni-4 wt%Sn). The Vickers hardness was found to increase with the hardening aging time due to a microstructure change; an adhesive wear mechanism was reported through pin-on-disc wear tests [7].

During sliding of two materials, the high shear force causes plastic deformation at the interacting surfaces, and a transfer layer is commonly formed which correlates with the friction and wear behaviour [8, 9, 10]. Rigney and co-workers studied the structure and chemical composition of the layer for at the

contact between a Ni-40wt%Cu block and 440C stainless steel [11, 12]. The transfer layers were found to be a few microns thick and consist of nanocrystalline grains. It was also reported that the loose wear debris was generated from the transfer layer in sliding [11]. Later, by studying the transfer and mixing layer developed between a bronze pin sliding against a brass disc, Rigney concluded that the sliding wear mechanism involves the development of a substructure deformation which leads to transfer, chemical reactions, mechanical mixing and fracture of ductile materials [13]. Godet et al. [14] reported that a transfer layer that is composed of 'third bodies' can be created, destroyed and regenerated while the layer flows and transmits load, accommodating velocity gradients.

In dry sliding condition, the friction and wear behaviour of CuNiSn alloy has been studied by several researchers [15-19]. Singh et al. [15, 19] assessed the cross-section of CuNiSn in the worn region after dry sliding against 440C stainless steel disc in air and flowing Argon gas through TEM. Distinct nanocrystalline sublayers (mechanically mixed layers, MML) on the pin worn surface were observed and linked to the friction and wear behaviour of the alloy. The top MML was generated due to the compaction and mixing of materials from contacting bodies, which was claimed to improve the wear resistance of the alloy [19]. Cai et al. [16] qualitatively correlated the friction and wear of a CuNiSn alloy pin to the microscopic crystallographic textures and the texture transition in the dry sliding against a bronze disk. Zhang et al. [20] studied the friction of an induction heating manufactured CuNiSn alloy when slid against GCr15 bearing steel lubricated with engine oil, and found that the friction was not affected by the aging time and the wear resistance was enhanced.

Although the friction and wear mechanisms of CuNiSn bronze alloy has been widely investigated, these studies were conducted with dry sliding under room temperature. However, in most applications, particularly heavy duty, lubrication of the bronze component is usually required with either oil or grease. In particular, in many tribology systems, the CuNiSn component needs to be operated in a high temperature environment. Nevertheless, the friction and wear mechanism of the CuNiSn bronze alloy under these conditions has yet to be determined. The aims of the study were therefore to investigate the friction and wear properties of the CuNiSn with grease lubrication under both room and elevated temperature, through a ball-on-disc contact configuration and using micro/nano-scopic techniques, including optical microscopy, SEM, EDX, TEM and nano-indenter.

2. Experimental method

2.1 Wear tests

Reciprocating friction and wear tests using a ball-on-disc configuration and conforming to ASTM G133, were conducted on a UMT-Tribolab testing platform with a REC-400 heating chamber (Bruker Corporation, USA).

During the testing, an alumina ceramic ball (Al_2O_3, from Atlas Ball and Bearing Co. Ltd, UK) with grade 25, a diameter of 4 mm, elastic modulus of 407 GPa, Vickers hardness of 1365 Hv, Poisson ratio of 0.21 was reciprocated against a static wrought and spinodally hardened CuNiSn bronze (ToughMet 3 AT 110, from Materion Corporation, USA, henceforth referred to as CuNiSn) disc. The alumina ball was held in a chuck and loaded against the CuNiSn disc. Instead of stainless balls, the alumina ball was used in the present study in order to minimise material transfer onto the testing specimens due to its inert counterface.

For CuNiSn sample preparation, 3 mm thick discs were sliced from a diameter of 25.4 mm bar using electrical discharge machining (EDM). In order to obtain identical testing surfaces, each disc was ground with SiC paper from 1200 to 4000 grit following by buff polishing with 1 and 0.25 µm diamond suspensions, leaving a surface roughness of R_a = 0.2 µm. From this process, at least 200 µm material from the surface was removed in order to get rid of the possible damaged layer caused by the EDM

1 slicing. New specimens (fresh balls and discs) were used for each test and cleaned in an isopropanol
2 ultrasonic bath prior to the test.

3 The reciprocating tests were conducted at both room temperature and elevated temperature of 110 °C
4 and lubricated by AeroShell Grease 64 (5 wt% of MoS_2, Shell PLC, UK). The lubricant grease had a
5 viscosity of 14.2 cSt at 40 °C and 3.4 cSt at 100 °C, and a range of operating temperature from -73°C
6 to +121 °C. The AeroShell Grease 64 was chosen because it is a widely used lubricant in severe
7 operating conditions for which CuNiSn is designed, i.e. aircraft bearing systems. Prior to the sliding
8 test, a thin layer of grease was evenly spread on top of the CuNiSn disc. In the high temperature tests,
9 a REC-400 heating chamber was used to heat up the contact before the sliding test taking place. Test
10 conditions are summarised in Table 1.

11

Table 1. Reciprocating sliding test conditions

Normal load	Stroke distance	Sliding speed	Testing duration	Ball material	Ball diameter	Disc material	Temperature
P = 1, 4 N	4 mm	20 mm/s (2.5 Hz)	90 min (13500 cycles)	Al_2O_3	4 mm	CuNiSn	Room temperature and 110 °C

12 For each test, the total reciprocating cycles were 13500 which produced a sliding distance of 108 m.
13 Based on the material mechanical properties, the initial mean Hertz contact pressures were 582 and 924
14 MPa at P = 1 and 4 N respectively. Each test was repeated once.

2.2 Characterization

16 The general morphology and microstructure of the worn surfaces were characterized using an Inspect
17 F FEG scanning electron microscopy (SEM) (FEI, Netherlands) attached with an energy dispersive X-
18 ray (EDX) detector. Dimensions of wear tracks, including 3D morphology, wear scar depth and wear
19 volume loss were assessed using optical microscopy (Alicona InfiniteFocusSL from Alicona Imaging
20 GmbH, Graz, Austria).

21 Focused ion milling (FIB) (FEI Quanta 200 3D SEM/FIB the Netherlands) and transmission electron
22 microscopy (TEM) were undertaken to investigate the cross-section of the worn surface. FIB milling
23 was undertaken using an FEI Helios G4 Nanolab (FEI, the Netherlands). Platinum deposition was
24 applied on the region of interest to prevent Ga^+ implantation and sputter erosion of the top portion of
25 the surface. TEM observation was obtained using a JEOL JEM-F200 (JEOL, Tokyo, Japan) operated
26 in STEM mode at 200 kV.

27 Nano indentation (Bruker Hysitron TI Premier, USA) equipped with a standard Berkovich diamond
28 indenter was used for nano-hardness measurement of the worn surfaces. An array of twenty nano
29 indentions was performed at 2 mN load (indentation depth around 110 nm) and intervals of 10 µm
30 between indentations.

3 Results and discussion

3.1 Friction and wear behaviour

33 Fig. 1 shows coefficient of friction, CoF of CuNiSn evolution with reciprocating cycles for various test
34 conditions. The sliding test showed two stages, a break-in or running-in stage during which CoF was
35 significantly changing, and a steady-state regime in which the average CoF and wear data were roughly
36 constant. The inset figures show the variance of CoF during running-in due to the breakdown of the
37 oxide layer formed on the polished surfaces prior to the test. Apparently, this breakdown was
38 accelerated by higher load and temperature. At P = 4 N, the CoF reaches steady-state rapidly, with
39 comparable values, 0.13 at room temperature and 0.135 at 110 °C. While for P = 1N, the CoF at 110 °C
40 at the steady state was found to be 0.15, which was 1.4 times that at room temperature. Regarding the
41 influence of the normal load, the CoF was found to be increased from 0.11 under 1 N to 0.13 under 4
42 N at room temperature. At 110 °C, the CoF decreased with load, from 0.15 to 0.135 which was
43 comparable to that at room temperature. This indicated that the interface that governed the frictional

1 behaviour of the countering materials may have different properties caused by varying operating
2 parameters, i.e. load, temperature. Post-test analysis towards the wear track, described later, provides
3 further information.
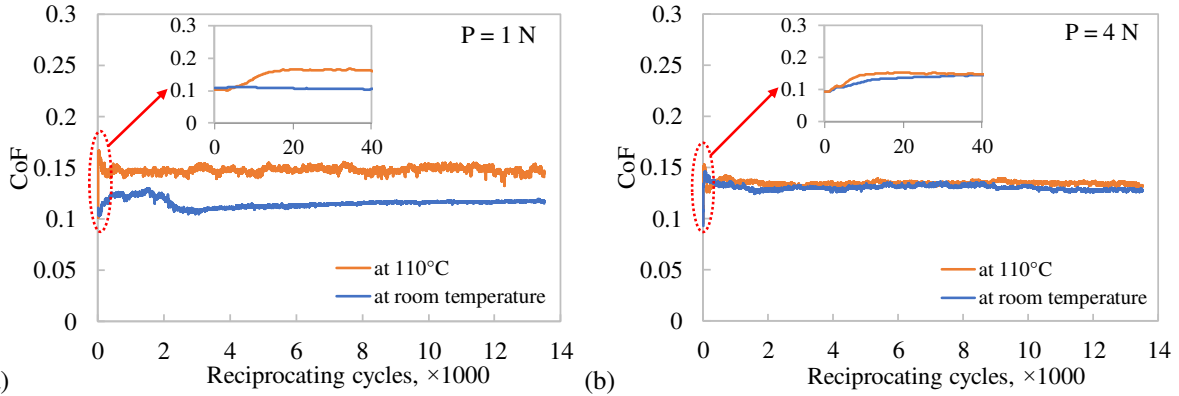
4 (a)   (b)

5 Fig. 1 CoF between alumina ball and CuNiSn disc under loads of (a) *P* = 1N and (b) *P* = 4 N, at both room
6 temperature and 110 °C

7 After the wear test, the CuNiSn disc and the countering alumina ball were cleaned using isopropanol to
8 remove remaining grease for optical and electron microscopy. Three-dimensional wear scar profiles
9 were measured using the Alicona microscope for quantifying the wear volume. The cross-section profile
10 of the worn surface perpendicular to the sliding direction is shown in Fig. 2. It is evident that the wear
11 of CuNiSn was influenced by both load and temperature. Higher load and temperature resulted in severe
12 operating conditions which deteriorated the interface between the CuNiSn disc and the alumina ball.
13 The largest wear scar was produced under 4N and elevated temperature, as shown in Fig. 2 (b). After
14 cleaning there was no surface damage or wear observed on the alumina ball by using the optical
15 microscope.
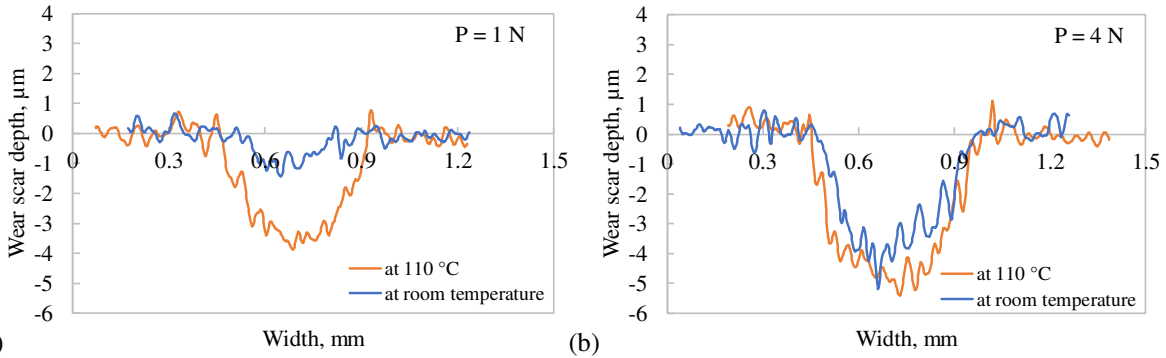
16 (a)   (b)

17 Fig. 2 Wear scar profiles on the CuNiSn discs measured by Alicona for (a) *P*=1N and (b) *P*=4 N, at both room
18 temperature and 110 °C

19 Specific wear rates *W*, in *μm³/Nm*, were calculated using:

$$W = \frac{V}{Pvt} \tag{1}$$

21 Where *V* is the wear volume loss, in µm³, *P* is the normal load, in N, and *v* is the sliding speed, in m/*s*
22 and *t* is the test duration, in s.

23 Resulting CoF, wear scar dimensions and specific wear rate are summarised in Table 2. The specific
24 wear rate was found to increase with load at room temperature but decrease at elevated temperature.
25 For all the conditions considered, the lowest specific wear rate was found to be 0.27×10^4 µm³/Nm at
26 room temperature while the highest was found to be 1.53×10^4 µm³/Nm at 110 °C, both of which
27 occurred at *P* = 1N. This agrees with the CoF values from the same testing conditions. The results
28 indicated that under the moderate load, the temperature affected the interface dominantly. This is

4

because the grease viscosity and the temperature are inversely proportional, i.e. the higher the temperature the lower the viscosity and hence the thinner the lubricating film. Consequently, friction was found to be higher at P = 1 N, 110 °C, as shown in Fig. 1 (a). In contrast, under higher load, P = 4 N, a lubricant layer was hardly formed at the interface no matter what the temperature was. In this case, the interface was mainly influenced by the load. Consequently, the friction (Fig 1. (b)) and wear scar profile (Fig 2. (b)) showed little difference between the two testing temperatures.

Table 2. Wear track dimensions and specific wear rate for varying testing conditions

Environment	Coefficient of friction	Wear scar width, µm	Wear scar depth, µm	Wear volume, µm^3, ×10^6	Specific wear rate, µm^3/Nm, ×10^4
Room temp, 1N	0.11	300	1.4	0.29	0.27
Room temp, 4N	0.13	590	5.2	2.02	0.47
110 °C, 1N	0.15	480	3.9	1.65	1.53
110 °C, 4N	0.134	600	5.4	2.72	0.63

3.2 SEM characterization of the worn surface

To evaluate the friction and wear mechanism between the CuNiSn disc and alumina ball, morphology and microstructure of the wear tracks were further characterized post mortem. Fig. 3-6 show SEM images of wear tracks on the CuNiSn disc after 13500 cycles of rubbing under varying loads and temperatures. Prior to SEM examination, the CuNiSn disc surface was ultrasonically cleaned with isopropanol. As the characterization of the used grease was not considered in the current study, the grease mixed with wear debris was removed prior to the cleaning process.

The SEM micrographs show that the microstructure of the wear track varied along its length, i.e. from the track end to the mid zone of the track. During sliding, transferred material was pushed to the side of the track mainly in the sliding direction, similar to snow shovelling. At the track end reversals transferred material accumulated. In addition, from Fig. 3 and 4 it can also be seen that the morphologies of worn surfaces were significantly different under the two testing temperatures. At 110 °C, wear debris was accumulated at the end of the track (Fig. 3 (c)), while under room temperature, sparse oxidation zones (dark regions in Fig. 3 (a) and (b)) were observed on the worn surface. Wear debris in Fig (3) showed evidence of more material transfer caused by plastic deformation of the surface material. Moreover, at the middle of the wear track (Fig.4), fine uniform wear furrows were seen on the wear track rubbed under 110 °C (Fig. 4 (b)) whilst a large sized groove was observed at room temperature. This indicated that temperature played an important role on the contact interface properties, and that the abrasion of wear debris, working as 'third body', was the main wear mechanism for the tests under 1N and room temperature.
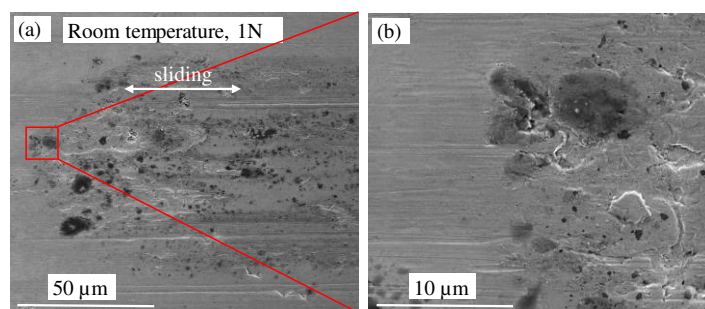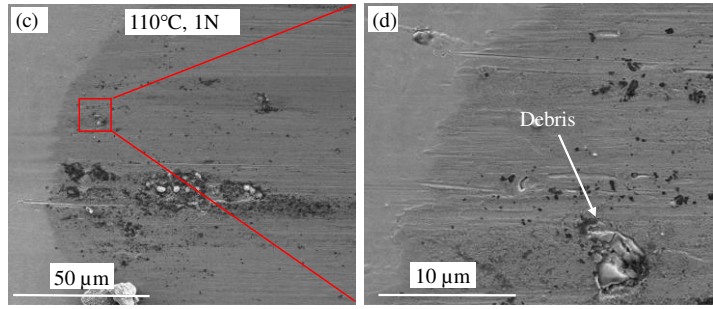
Fig. 3 SEM images showing the top view of the end-stroke wear tracks and detailed microstructure at P = 1N, and (a) & (b) at room temperature, (c) & (d) at 110 °C
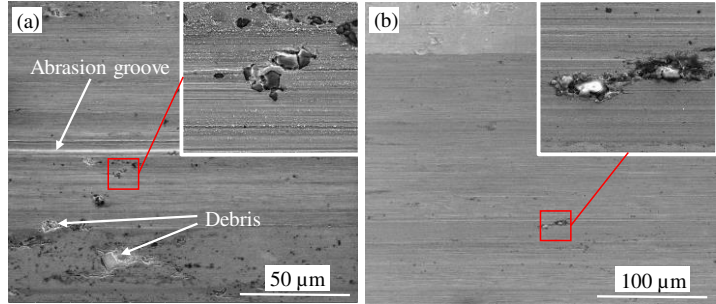
Fig. 4 SEM images showing the top view of the mid-stroke wear tracks and detailed microstructure at P = 1 N, and (a) at room temperature, (b) at 110 °C

Fig. 5 and 6 show the microstructure and chemical composition of wear tracks subjected to P = 4N and varying temperature. It is apparent that higher load produced larger sized wear tracks and the abrasive wear mechanism dominated. Slip lines were observed on the un-worn surface near the edge of the wear track, as shown in Fig. 5 (c) and (f). This was due to the synergistic effects of the high normal and shear stresses occurred at the interface. Detailed composition information for specs 1 and 2 on Fig. 5(d) are shown in Tables 3. According to the EDX maps and point analysis shown in Fig. 5(b), (e), and Table 3, the wear track was predominantly covered by an oxide layer. Bronze alloy elements Cu, Ni and Sn were found to be distributed over both fresh and worn surfaces of the CuNiSn disc. Distribution of S and Mo elements from solid lubricant additives in grease were found to be distinguished from fresh surface which were mechanically mixed in the top layer on the wear track.
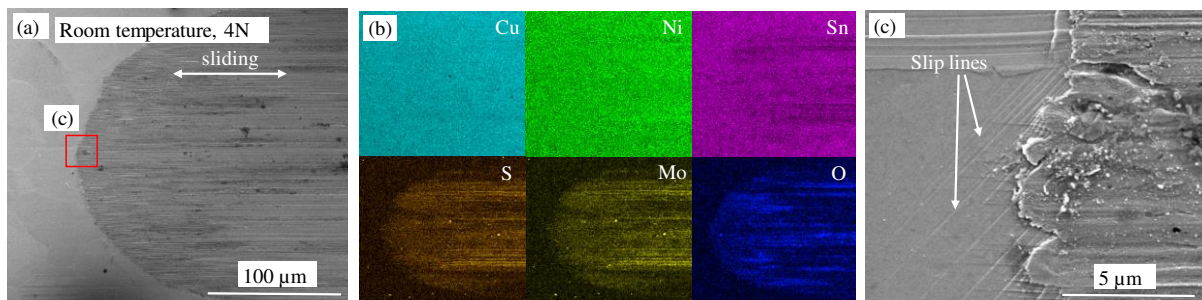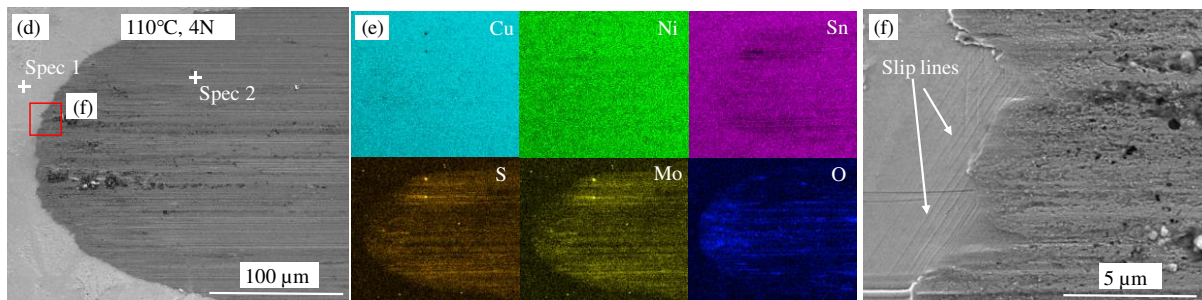
Fig. 5 SEM images showing the microstructure and EDX mapping of the chemical elements distribution for the end-stroke wear track at P = 4 N, (a) (b) (c) at room temperature, and (d) (e) (f) at 100 °C
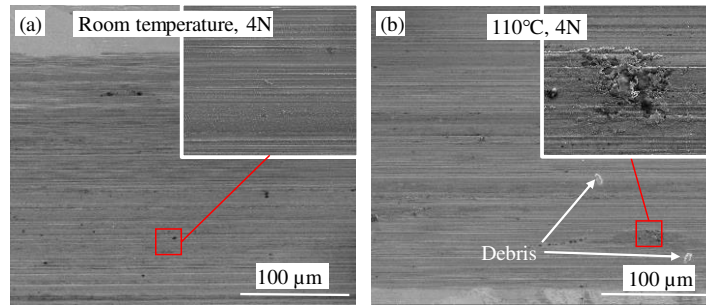
Fig. 6 SEM image showing the mid-stroke wear track and the microstructure at P = 4 N, (a) at room temperature, and (b) at 100°C

Table 3. EDX point analysis of chemical composition (At %) for points Spec 1 and 2 (shown in Fig. 5 (d)

Point	Cu	Ni	Sn	C	O	S	Mo
Spec 1	54.9	12	2.9	29.1	1.1	-	-
Spec 2	50	11	2.4	32.7	3	0.7	0.3

3.3 TEM characterization

While SEM characterization shows the micro-structure of the worn surface from the top, a cross-section analysis yields depth information for subsurface material deformation and formation of the transfer layer, which is critical to reveal the wear mechanism.

Fig. 7 shows the TEM micrographs of the wear track cross-section on the CuNiSn disc after 13500 cycles at both room temperature and 110 °C. Compared to the fresh subsurface (Fig.7 (a)), an influenced layer right beneath the Pt coating were observed capping on the wear track at both test temperatures, which is known as a tribolayer. The thickness of the capping layer generated at room temperature was 1-1.5 µm (Fig.7 (b)) compared with 200-300 nm for 110 °C (Fig.7 (c)). A deformation substructure was seen on the cross-section for both testing temperatures after 13500 cycles. A similar deformation layer was observed in a previous study by Singh et al. [15], in which a CuNiSn bronze pin was slid against a stainless steel disc without lubrication and under room temperature. The capping layer formation process involves deformation, transfer, chemical reaction, and mechanical mixing [21], and therefore determined the friction and wear behaviours of the CuNiSn.
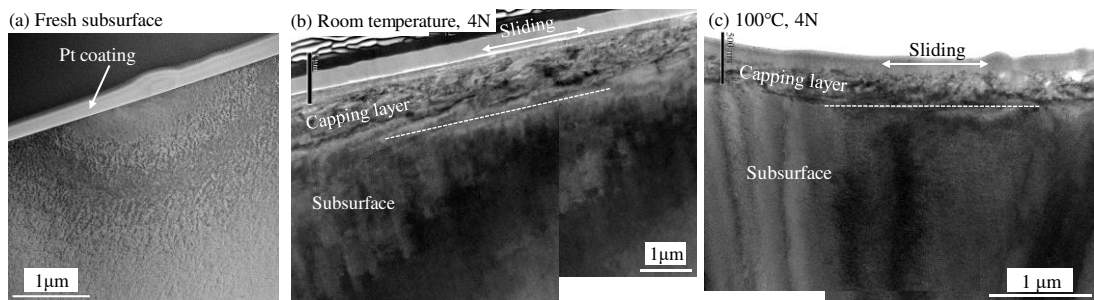
Fig. 7 Bright field cross-section TEM micrographs, (a) fresh subsurface, (b) and (c) formation of a capping layer in the immediate vicinity of the surface at room temperature and at 100 °C testing temperatures respectively

Fig.8 (a) shows the bright field cross-section microscopy of the CuNiSn wear track and provides tribolayer details at room temperature and P = 4 N. Two sublayers beneath the surface within the tribolayer were observed, as shown in Fig. 8 (b). The top layer close to the surface is a thinner, fine-grained mixed material that is denoted as a mechanically mixed layer (MML), with a thickness of approximately 200 nm (Fig. 8(b)). It is reported that this layer has a different composition from that of the bulk material [21, 22, 14]. This MML separated the direct contact between CuNiSn and the alumina ball, transmitting load and accommodating the shear velocity gradients along the interface. It was

generated during sliding and could be destroyed and regenerated [14]. Fig.8 (c) shows the EDX mapping of Fig. 8 (b), revealing the chemical composition of the MML. Chemical elements S and Mo were from the additives in the lubricant grease. The environmental source, lubricant grease in this work became a source of chemical species that were incorporated in the MML. An even thinner O-rich layer was observed stacking on top of the MML, shown as a narrow dark zone in Fig. 8 (b). This may be due to metal oxidation occurring on the worn surface in the post-test cleaning process. During the sliding test, the CuNiSn surface was covered with grease, shielded from the reactive environment, so the oxidation process was prevented. The plastically deformed layer (PDL) was right below the MML in the base material. A clear demarcation was observed between the deformation substructure of PDL and the MML, shown in dark field cross-section image (Fig. 8 (b)). A fine-grained sublayer PDL was made of nanograins elongated along the sliding direction. By comparison TEM examination, Singh et al. reported that the grains were heavily deformed, indicating large strain had been experienced by the sublayer during the sliding wear test [15]
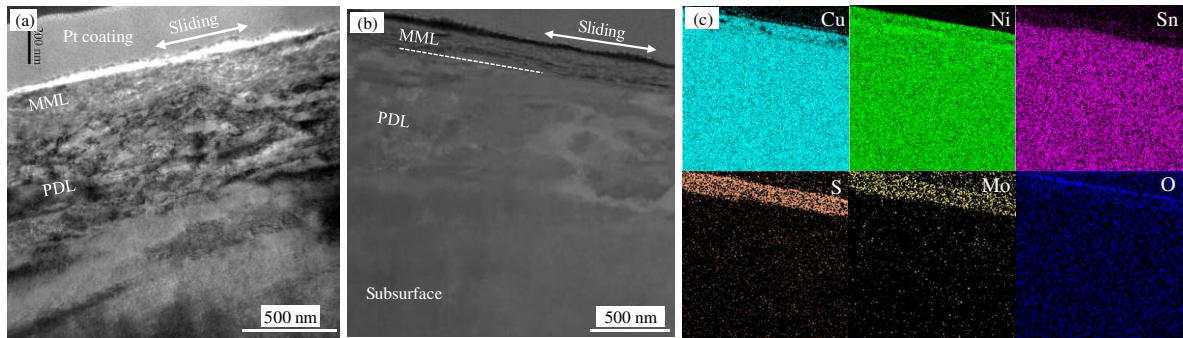
Fig. 8 TEM micrographs showing details of the capping layer at room temperature and P = 4 N, (a) bright field cross-section (b) dark field cross-section in the adjacent region of (a), and (c) EDX mapping showing the chemical elements distribution in (b)

Fig.9 shows the bright and dark field microscopies of the cross-section of the wear track under 110 °C and P = 4 N. In contrast to the room temperature case, the MML was barely observed in the TEM micrographs as there was no boundary presented against the PDL. The overall deformed layer was much smaller than that under room temperature (Fig. 8). It can be concluded that the tribolayer, especially the MML was hardly developed or easily destroyed on the wear track during sliding at 110 °C. As the behaviour of this layer depends on the dimensions, compositions and properties, it can be beneficial or harmful to the friction and wear of the material. Indeed, as shown in Fig.1-2 and Table 2, CuNiSn demonstrated lower friction and higher wear resistance at room temperature than at 110 °C. This is probably due to the fact that the tribolayer was more efficient in reducing friction and wear at room temperature than 110 °C for the CuNiSn and Al_2O_3 tribolo-system.
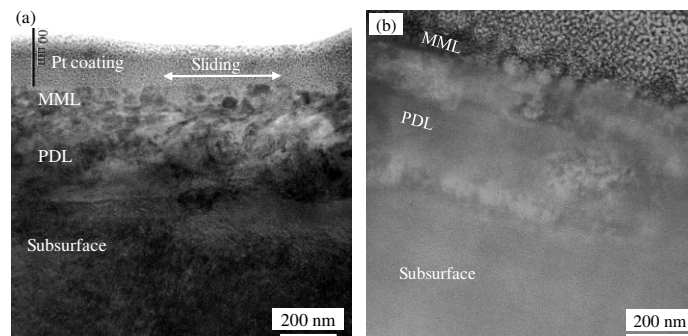
Fig. 9 TEM micrographs showing details of the capping layer at 110 °C and P = 4 N, (a) bright field cross-section (b) dark field cross-section in the adjacent region of (a)

Fig. 10 shows the schematic diagram of the tribolayer in the sliding contact between the alumina ball and the CuNiSn. The operating conditions, temperature, load and lubricant, determined the formation and rupture of the tribolayer. The lubricating grease helped to separate the contacting surfaces, and

introduced the solid lubricant MoS$_2$ particles which contributed to friction and wear reduction. In reciprocating rubbing, abrasive wear debris from the CuNiSn together with the MoS$_2$ particles were mechanically mixed and stacked on top of the plastic deformed layers, such as MML and PDL shown in Fig. 10. Therefore, it is concluded that the friction and wear of the CuNiSn bronze is largely influenced by the formation/rupture of the tribolayer.
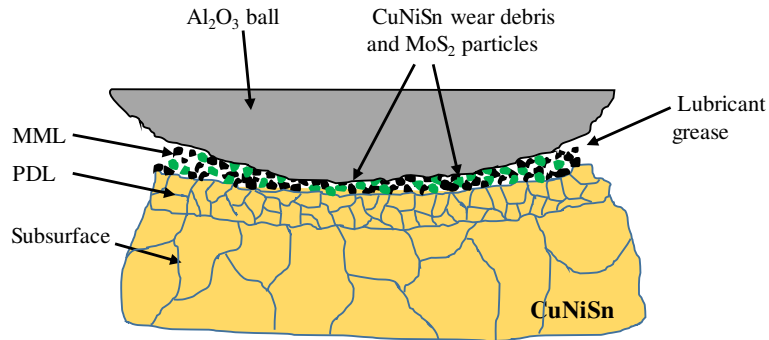
Fig. 10 Schematic diagram of the tribolayer between alumina ball and CuNiSn bronze under sliding friction

3.4 Nano-indentation hardness

To study the mechanical property of the tribolayer generated on the CuNiSn surface, the nano-hardness was measured with a Bruker's Hysitron TI Premier Nanoindenter. Twenty nano-indentations were performed along the central line of each wear track, as shown in Fig. 11 (a). The interval between indents was 10 μm so a total length of 190 μm of the wear track was measured. The instrumented indentation method built in the nano-indenter provided a continuous record of the variation of indentation load as a function of the penetration depth. Fig. 11 (b) shows the typical load-depth curves for varying testing conditions. From the load-depth curve, the individual hardness of each indent was analysed using the Oliver and Pharr method [23, 24], which was incorporated in the analysis program on the nano-indenter. The average hardness from the twenty indents is shown in Fig. 11 (c).

From Fig.11 (b) it can be seen that the indentation depth for different testing conditions varied from 105 to 115 nm. These depths were comparable to the thickness of the MML on the wear track from the TEM micrograph (Fig.8 and 9) and so relate to the properties of the MML and not the substrate. Worn surfaces had a lower nano-hardness compared with the fresh one. At 1N load, after 13500 cycles, the surface hardness of the worn surface showed an approximate 8% reduction compared to that of the unworn surface. At room temperature, the nano-hardness was 5.05 GPa at P = 1N and 4.77 GPa at P = 4 N, compared to 4.97 GPa and 4.74 GPa at 110 °C. In sliding, the unworn CuNiSn surface with higher hardness was deteriorated and incorporated with material transfer and mechanical mix. Apparently, the top layer composed of loose particles and debris demonstrated a lower nano-hardness at both test temperatures. However, a slightly higher nano-hardness under room temperature was associated with a better wear resistance compared to that at 110 °C (lower specific wear rate in table 2). The mixed material on the surface, seen as elevated plateaux, softer than the fresh surface material, played an important role in determining the wear property of CuNiSn. Due to the limited nano-indentation depth, there is no indicative parameter that can be used to analyse the mechanical property from the lower layer, PDL, or even deeper to the subsurface of the bulk material. However, as the microstructure size was found to be decreased in PDL, it suggested that the micro-hardness in this layer was greater than with the subsurface, similar to the process of mechanical hardening [25, 26].
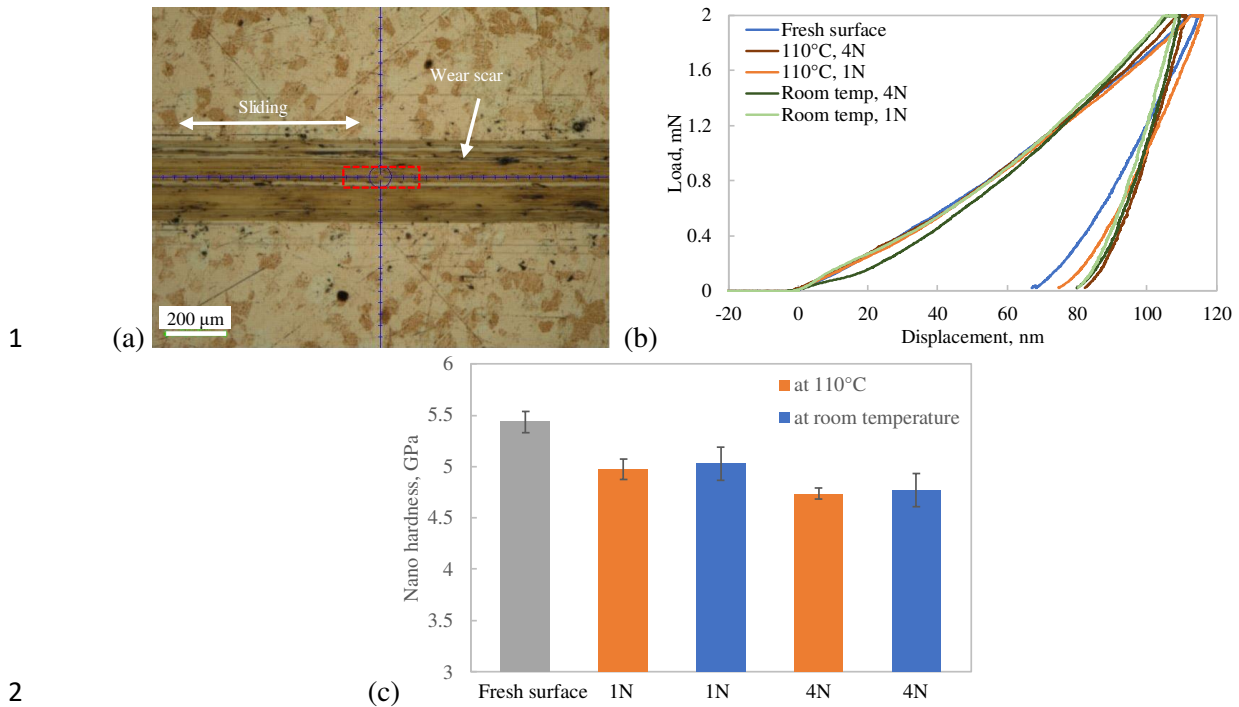
Fig. 11 (a) Location of nano-indentations, (b) typical nano-indentation load-depth curves for varying conditions (one curve selected from 20 for each testing condition), and (c) Nano-hardness of wear track on the CuNiSn bronze

4 Conclusions

CuNiSn bronze was experimentally studied using a ball-on-disc reciprocating sliding configuration against alumina ball under varying operating conditions and environments. Friction and wear resistance were analysed using post-test techniques, including Alicona optical microscopy, SEM, TEM and nano-indenter. Conclusions from the study are summarized as follows:

- The coefficient of friction, CoF, of CuNiSn bronze was influenced by the environmental temperature. Under 1N normal load, the CoF at the steady stage was 0.15 at 110 °C compared to 0.11 at room temperature. Both the load and temperature had significant influences on the bronze's CoF.

- The wear resistance of CuNiSn reduced at elevated temperature. Under 1N load, the specific wear rate was 1.53×10^4 $\mu m^3/Nm$ at 110 °C compared with 0.27×10^4 $\mu m^3/Nm$ at room temperature.

- The wear mechanisms of CuNiSn against the alumina ball were investigated with SEM characterization. The chemical elements S and Mo from the grease additives were found to be mechanically mixed in the top layer of the wear track.

- Microscopic view of the cross-section for the CuNiSn wear track was measured with a TEM. The tribolayer of deformed material beneath the wear track surface was found to be 1-1.5 μm at room temperature and 200-300 nm at 110 °C. Two sublayers, MML and PDL were observed with different structures and compositions.

- Nano hardness of the wear track on the worn CuNiSn surface decreased by 8% compared to that on the fresh surface. The EDX mapping confirmed that the top layer on the wear track was composed of wear debris, oxidation and lubricant materials that were mechanically mixed and layered on the wear track. This tribolayer governs the friction and wear of CuNiSn bronze in sliding against an alumina counterface.

Acknowledgement

Reference

[1] Materion Brush Ltd., US. Available online: https://materion.com/products/high-performance-alloys/toughmet (accessed 1 February 2020).

[2] W.R. Cribb, F.C. Grensing, Spinodal copper alloy C72900 - new high strength antifriction alloy system, Canadian Metallurgical Quarterly, 50(3) (2011), 232-239. https://doi.org/10.1179/1879139511Y.0000000012

[3] W.R. Cribb, Copper spinodal alloys for aerospace, Advanced Materials & Processes, ASM International, 6 (2006), 44.

[4] W.R. Cribb, M.J. Gedeon, F.C. Grensing, Performance advances in copper-nickel-tin spinodal alloys, Advanced Materials & Processes, ASM International, 9(2013), 20-25.

[5] D.K. Jr., W.R. Cribb, Toughmet alloy: improving thrust bearing performance through enhanced material properties, SAE Commercial Vehicle Engineering Congress and Exhibition Chicago, Illinois October 26-28, 2004. https://doi.org/10.4271/2004-01-2675

[6] A.V. Samant, M.J. Gedeon, R.E. Kusner, C.A. Finkbeiner, F.C. Grensing, W.R. Cribb, Properties of ToughMet® 3 copper-nickel-tin alloy for oxygen enriched atmosphere applications, ASTM 14th International Symposium on Flammability and Sensitivity of Materials in Oxygen-Enriched Atmospheres, San Antonio, TX, US. 2016, 296-307. https://doi.org/10.1520/STP159620150069

[7] S. Ilangovan, J. Sreejith, M. Manideep, S. Harish, An experimental investigation of Cu-Ni-Sn alloy on microstructure, hardness and wear parameters optimization using DOE, Tribology in Industry, 40(1) (2018), 156-163. https://doi.org/10.24874/ti.2018.40.01.15

[8] W.M. Rainforth, R. Stevens, J. Nutting, Deformation structures induced by sliding contact, Philosophical Magazine A, 66(4) (1992), 621-641. https://doi.org/10.1080/01418619208201580

[9] J.M. Bailey, A.T. Gwathmey, Friction and surface deformation during sliding on a single crystal of copper, ASLE Transactions, 5(1), 1962, 45-56. https://doi.org/10.1080/05698196208972452

[10] W.M. Rainforth, A.J. Leonard, C. Perrin, A. Bedolla-Jacuinde, Y. Wang, H. Jones, Q. Luo, High-resolution observations of friction-induced oxide and its interaction with the worn surface, Tribology International, 35 (2002), 731-748. https://doi.org/10.1016/S0301-679X(02)00040-3

[11] P. Heilmann, J. Don, T.C. Sun, D.A. Rigney, W.A. Glaeser, Sliding wear and transfer, Wear, 91 (1983), 171-190. https://doi.org/10.1016/0043-1648(83)90252-1

[12] D.A. Rigney, L.H. Chen, M.G.S. Naylor, A.R. Rosenfield, Wear processes in sliding systems, Wear, 100 (1984), 195-219. https://doi.org/10.1016/0043-1648(84)90013-9

[13] D.A. Rigney, Transfer, mixing and associated chemical and mechanical processes during the sliding of ductile materials, Wear, 245 (2000), 1-9. https://doi.org/10.1016/S0043-1648(00)00460-9

[14] D. Dowson, The third body concept: interpretation of tribological phenomena, Proceedings of the 22nd Leeds-Lyon Symposium on Tribology, the Laboratoire De Mécanique Des Contacts, Institut National Des Sciences Appliquées De Lyon, France, 5th-8th September 1996.

[15] J.B. Singh, W. Cai, P. Bellon, Dry sliding of Cu-15 wt%Ni-8 wt%Sn bronze: Wear behaviour and microstructures, Wear, 263 (2007) 830-841. https://doi.org/10.1016/j.wear.2007.01.061

[16] W. Cai, J. Mabon, P. Bellon, Crystallographic textures and texture transitions induced by sliding wear in bronze and nickel, Wear, 267 (2009) 485-494. https://doi.org/10.1016/j.wear.2008.11.016

[17] S. Zhang, B. Jiang, W. Ding, Dry sliding wear of Cu-15Ni-8Sn alloy, Tribology International, 43(2010), 64-68. https://doi.org/10.1016/j.triboint.2009.04.038

[18] J. Weninger, J.A. Bares, T. Tyler, J. Ye, P. Bellon, Microstructural evolution in cu-spinodal alloy driven by high-energy ball milling and dry sliding wear, Proceedings of Solid to Solid Phase Transformations in Inorganic Materials 2005, Eds. J. M. Howe et al., 887-892.

[19] J.B. Singh, J.-G. Wen, P. Bellon, Nanoscale characterization of the transfer layer formed during dry sliding of Cu-15 wt.% Ni-8 wt.% Sn bronze alloy, Acta Materialia, 56 (2008), 3053-3064. https://doi.org/10.1016/j.actamat.2008.02.040

[20] S. Zhang, B. Jiang, W. Ding, Wear of Cu-15Ni-8Sn spinodal alloy, Wear 264 (2008), 199-203. https://doi.org/10.1016/j.wear.2007.03.003

[21] D.A. Rigney, M.G.S. Naylor, R. Divakar, L.K. Ives, Low energy dislocation structures caused by sliding and by particle impact, Materials Science and Engineering, 81(1986), 409-425. https://doi.org/10.1016/0025-5416(86)90279-X

[22] X.J. Wang, D.A. Rigney, Sliding behavior of Pb-Sn alloys, Wear, 181-183 (1995), 290-301. https://doi.org/10.1016/0043-1648(95)90036-5

[23] G.M. Pharr, W.C. Oliver, Measurement of thin film mechanical properties using nanoindentation. MRS Bulletin, 17(7) (1992), 28-33. https://doi.org/10.1557/S0883769400041634

[24] W.C. Oliver, G.M. Pharr, An improved technique for determining hardness and elastic modulus using load and displacement sensing indentation experiments, Journal of Materials Research, 7(6) (1992) 1564-1583. https://doi.org/10.1557/JMR.1992.1564

[25] D. Kuhlmann-Wilsdorf, The theory of dislocation based crystal plasticity, Philisophical Magazine A, 79(1999), 955-1008. https://doi.org/10.1080/01418619908210342

[26] N. Hansen, X. Huang, D.A. Hughes, Microstructural evolution and hardening parameters, Materials Science and Engineering: A, 317(2001), 3-11. https://doi.org/10.1016/S0921-5093(01)01191-1